

# Simulation of a Gas-Solid Flow Field in a Two-Stage Rice Husk High-Temperature Pyrolysis and Gasification Cyclone Gasifier

Ming Zhai,\* Yu Zhang, Tiezhu Ge, Peng Dong, and Cuijing Zhao

A scheme for using a two-stage cyclone gasifier for high-temperature rice husk pyrolysis and gasification to reduce the tar content in biogas is presented in this study. The two-stage cyclone gasifier consisted of an upper cyclone high-temperature pyrolysis chamber and a lower steam spray gasifier. The staging pyrolysis and gasification process used in this study can increase the carbon conversion efficiency and reduce tar content by increasing the pyrolysis temperature. This process uses part of the produced gas for combustion in an external burner to generate high-temperature (1600 °C) anaerobic flue gas and to provide heat for pyrolysis and gasification. This study simulates the isothermal gas phase and the gas-solid flow field for the upper cyclone chamber, as well as the gas-solid flow field, with steam (heat transfer between the steam and the gas is considered), for the entire gasifier by varying the structural and operational parameters. The optimal parameters for the cyclone gasifier for good mixing and lengthy residence (2.3 to 4.8 s) of the rice husk particles were found to be inlet angles of 20° and 30° with inlet velocities between 40 and 80 m/s.

*Keywords:* Rice husk; High-temperature pyrolysis; Gasification; Two-stage cyclone gasifier; Gas-solid flow field; Numerical simulation

*Contact information:* Harbin Institute of Technology, Dongli Building, Room 422, 92 West Dazhi Street, Nangang District, Harbin, Heilongjiang Province, 150001, China;

\* Corresponding author: zhaiming@hit.edu.cn

## INTRODUCTION

Biomass gasification converts solid biomass into useful gases through thermochemical conversion (Basu 2010). The gaseous products can be used for producing power and for central heating. However, conventional biomass gasification uses a lean combustion process, which uses the heat from the flue gas for pyrolysis and gasification and can generate much tar (Loppinet-Serani *et al.* 2008). Tar is a complex mixture of condensable hydrocarbons, including, among others, oxygen-containing, 1- to 5-ring aromatic, and complex polyaromatic hydrocarbons (Basu 2010). Too much tar will pollute a gasifier's cylinders and can clog pipelines or gas orifices of downstream power generation unit operating with the produced gas and spark plugs of a stationary reciprocating engine generator using the produced gas. This will lead to abnormal operating conditions of power generation and gas supply. Post-gasification tar reduction usually employs washing, but this process contaminates water heavily. However, there are several options that are available for *in situ* tar reduction. These include modification of operating conditions such as temperature (Narváez *et al.* 1996; Devi *et al.* 2003), pressure (Knight 2000), gasification medium (Herguido *et al.* 1992; Kinoshita *et al.* 1994; Gil *et al.* 1999), residence time (Kinoshita *et al.* 1994), design of the gasifier (Susanto and Beenackers 1996; Milne *et al.* 1998; Knoef 2005), addition of catalysts (Sutton *et al.* 2001; Mastellone and

Arena 2008; Mettanant *et al.* 2009), and secondary oxygen injection for selective oxidation of the tar (Pan *et al.* 1999). High-temperature operation is the most efficient option; however, it may have a negative impact on the heating value of the produced gas as a result of increasing the temperature by means of more combustion. According to authors' previous work (Zhang *et al.* 2014), heat self-sufficiency of the staging pyrolysis and gasification process can be achieved by using 15.4% to 20.5% of the total produced gas for combustion. Therefore, more gas needs to be combusted, and there is less produced gas remaining (reduced by 5%), but the heating value of the gas increases due to there being more H<sub>2</sub> and CO generated.

Taking into account the significant physical and chemical properties of the chosen biomass fuel, as well as the examination of the process and conditions of tar generation (Knoef 2005), this paper presents a two-stage rice husk cyclone gasifier scheme for high-temperature pyrolysis and gasification to reduce the amount of tar generated in biogas. The process uses part of the produced gas for combustion in an external burner to generate a high-temperature anaerobic flue gas, as well as to provide heat for pyrolysis and gasification. The two-stage rice husk cyclone gasifier consists of an upper cyclone with a high-temperature pyrolysis chamber, and a lower steam spray gasifier.

The focus of this paper is on the two-stage rice husk high-temperature pyrolysis and gasification cyclone gasifier. A physical model was established at first, and then the gas-phase isothermal flow field of the upper, high-temperature pyrolysis chamber was simulated. The effects of different inlet angles on the axial velocity, tangential velocity, and pressure distribution of the isothermal flow field were investigated. The structural parameters (inlet style and its angle) for the pyrolysis of the rice husk particles with a uniform diameter of 1.3264 mm and a density of 500 kg/m<sup>3</sup> were approximately determined. After this, the rice husk particle phase was added, and the gas-solid two-phase flow field was simulated for the upper, high-temperature pyrolysis chamber. The effects of different injection velocities and injection angles on the mixing and escaping of rice husk particles were investigated. Finally, the steam injection was added to investigate the effects of the steam on the whole gas-solid flow field and to determine the basic structural and operational parameters of the two-stage rice husk cyclone gasifier.

## **Basic Structure of the Two-Stage Rice Husk High-Temperature Pyrolysis and Gasification Cyclone Gasifier**

### *The design scheme*

Figure 1(a) displays the basic structure of the two-stage rice husk high-temperature pyrolysis and gasification cyclone gasifier. The operation of the gasifier is explained in the rest of this paragraph. Part of the residual heat from the 1600 °C biogas generated by the cyclone gasifier was used to heat the compressed air to 800 °C. The compressed air was burned with a fuel (rice husk) within a high-speed gas-fired combustor. The flue gas with high temperature (greater than 1600 °C) and low oxygen content that was generated by the high-speed gas-fired combustor was injected into the upper cyclone pyrolysis chamber at high speed. Meanwhile, the rice husk feedstock was mixed and heated by the flue gas, and part of the fixed carbon content (the solid combustible residue that remains after a rice husk particle is heated, and the volatile matter is expelled) was gasified after the pyrolysis process. The other portion of the residual heat from the biogas mentioned above was used to heat the feed water, thus converting it into steam. The temperature of the steam was 425 °C. The steam was injected into the lower steam spray gasifier to gasify the residual fixed carbon. This procedure eliminated tar generation completely (Zhang *et al.* 2014).

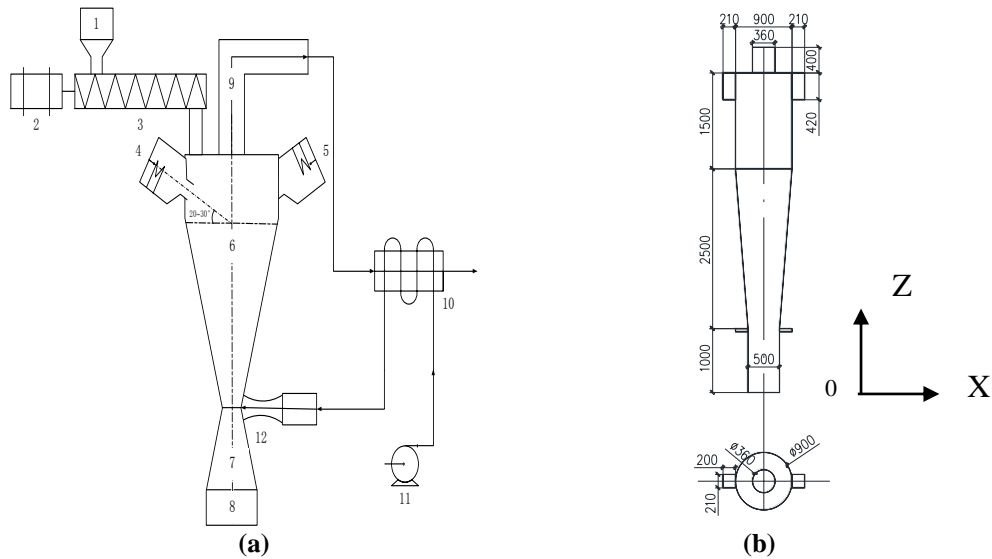


**Fig. 1.** Schematic diagram of the two-stage rice husk cyclone high-temperature pyrolysis gasifier. Components include: (1) Rice husk bunker, (2) Electrical motor, (3) Screw feeder, (4 and 5) High-speed gas-fired combustors, (6) Upper cyclone high-temperature pyrolysis chamber, (7) Lower steam spray gasifier, (8) Ash hopper, (9) Biogas discharge pipe, (10) Heat exchanger, (11) Water pump, and (12) Venturi tube

### Dimensions

Rice husk was selected as the fuel in this design. In a 1-MW internal combustion generator unit, the consumption of rice husk was 1200 kg/h, and the biogas production rate was 2680 Nm<sup>3</sup>/h in the cyclone gasifier. The composition of the produced gas was provided by the authors' previous work (Zhang *et al.* 2014), which demonstrated that the heating value of the gas is about 8500 kJ/m<sup>3</sup>. Without any other fuels, only 15.4% to 20.5% of the biogas was needed as fuel to maintain stable operations in the cyclone gasifier. The primary dimensions of the cyclone gasifier are shown in Fig. 1(b). The dimensions were determined to ensure that an adequate capture rate of char was maintained because char was necessary for reacting with the high-temperature steam. They were also determined to guarantee that the pyrolysis of the rice husk particles occurred and to guarantee that an optimal temperature (1200 °C and higher) was retained, which was vital for stable operation of the whole system and production of the biogas. Zhao provides detailed calculations in his research (2012).

## RESULTS AND DISCUSSION

### Meshing and Validation of the Turbulence Model

Based on the structure of the upper cyclone chamber, the Cooper meshing scheme (which treats the volume as consisting of one or more logical cylinders, each of which is composed of two end caps and a barrel) was used for the major hexahedron meshing combined with wedge and tetrahedron meshes, which is a combination of structured and unstructured grids (Zhao 2012).

According to previous studies, for a swirling flow field, the Reynold's stress model (RSM) has beneficial effects (Liu *et al.* 2003; Hu *et al.* 2004; Liu *et al.* 2005); thus, RSM was chosen for the simulation in this section. However, compared with other turbulence models, RSM considers the anisotropic properties of a flow. Therefore, the Reynolds stress

terms (six terms) must be added to the computations, which makes convergence more difficult. Thus, the renormalization group theory (RNG) model was used first for computing the gas-phase flow field until convergence was achieved. Then, the convergent data was used as the initial data for the RSM model computation to ensure that convergence had occurred. The main numerical methods used in this study were the semi-implicit method for pressure linked equations (SIMPLE) method (for pressure-velocity coupling computation), the second-order upwind scheme (for convective terms), and the pressure staggering option (PRESTO!) scheme (for pressure gradient terms). To validate the models chosen, the single-phase flow field computation data of a gas-solid cyclone separator was compared with the experimental data from the research of Fraser *et al.* (1997). The boundary conditions were velocity (7.5 m/s) for the inlet, outflow for the outlet (flow rate weighting = 1), outflow for the particle capture outlet, and no gas at the particle capture outlet (flow rate weighting = 0). The wall boundary condition was no-slip so that the standard wall function method could be used. FLUENT Software was used for the simulations, and the computer had a 2.8 GHz 4 core processor (CPU) and 12 GB of RAM.

Figure 2 shows a comparison of the computation and the experiment. The parameters are the axial and tangential velocity distributions at the cross section of  $X=0$  and  $Z=610$  mm. There was some difference between the RSM results and the experiment ones, especially at 0.02 to 0.05 r/m. Numerical diffusion and viscosity effects when solving the Navier-Stokes equations was responsible for the difference. Flows with a strong cross-grid component were particularly sensitive to them. However, the results still indicated the acceptability of using RSM for strong swirl turbulent flow field calculations.

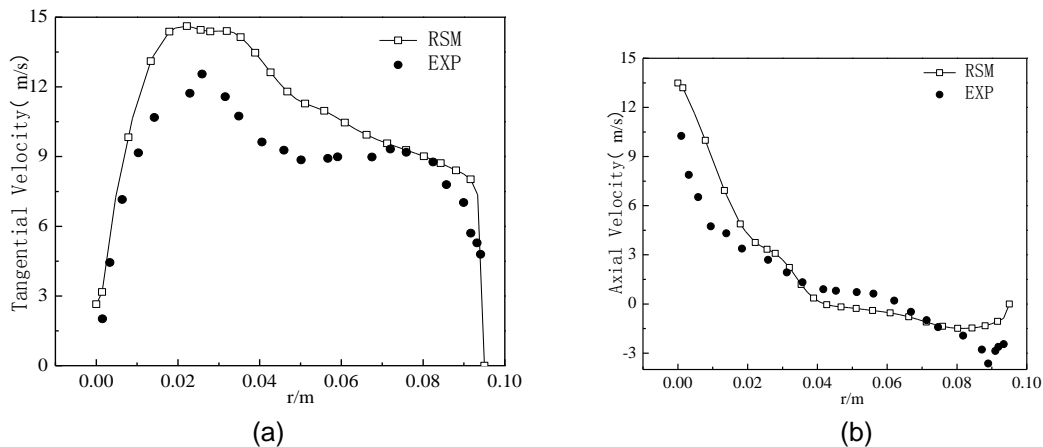


**Fig. 2.** Comparison of calculated (simulation) and experimental data: (a) experimental vs. calculated tangential velocities, (b) experimental vs. calculated axial velocities

### Gas Phase Isothermal Flow Field for the Upper Cyclone High-Temperature Pyrolysis Chamber

In Fig. 1(a), the flue gas was supplied through high-speed gas-fired combustors (4 and 5), and the biogas discharge pipe was 9. After the high-temperature flue gas flowed into the upper cyclone high-temperature pyrolysis chamber, since the biogas discharge pipe did not insert into the cyclone gasifier, it inevitably formed a short circuit flow, so the flue gas may have directly entered the biogas discharge pipe. However, a certain angle between the intake tube and the chamber would cause the flue gas to be propelled downward into the chamber by gravity and inertial force. In this way, the rice husk particles would stay in the chamber longer and would be able to complete pyrolysis. Because the temperature and the velocity of the flue gas were very high, the biogas discharge pipe did not extend to the

inside of the chamber. Double intake tubes were designed so that particular angles ( $0^\circ$ ,  $10^\circ$ ,  $20^\circ$ ,  $30^\circ$ ,  $40^\circ$ ,  $50^\circ$ , and  $60^\circ$ ) were achieved between the intake tube and the chamber. The high-temperature flue gas was replaced with air for simplification with an injection velocity of 80 m/s. The inlet velocity was determined by the high-speed combustor. The velocity of the falling rice husk particles was 0.05 m/s.

Figure 3(a) shows the axial velocity distributions at the cross section of  $X=0$  and  $Z=2000$  mm. The axial velocity increased with the radius of the cross section and reached a maximum at the center. Regardless of whether the inlets were tangential to the cylinder or not, the flow field in the chamber had two regions: an outer downward region and an inner upward region. The axial velocity at the interface of the two regions was zero. When the angle between the intake tube and the chamber was in the range of  $0^\circ$  to  $40^\circ$ , the maximum axial velocity was greater than it was for other inlet angles. Figure 3(b) shows the tangential velocity at the cross section of  $X=0$  and  $Z=2000$  mm. The maximum tangential velocity decreased as the angle between the intake tube and the chamber increased from  $0^\circ$  to  $60^\circ$ . This is because the tangential component of velocity became smaller as the angle between the intake tube and the chamber increased. When the angle between the intake tube and the chamber was between  $10^\circ$  and  $30^\circ$ , the maximum tangential velocity was larger and more symmetrical than it was for other inlet angles, which indicated that the gas phase was well-mixed. The velocity profiles were almost asymmetric because the inlets were asymmetric.

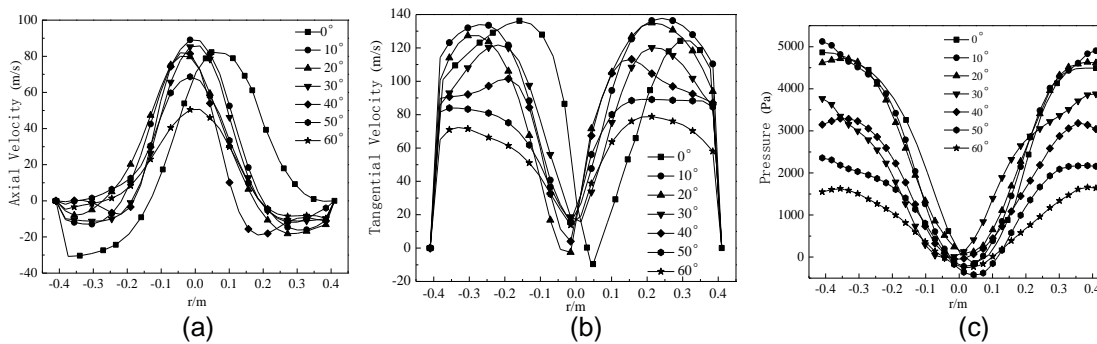


**Fig. 3.** Velocity and total pressure distribution at the cross section of  $X=0$  and  $Z=2000$  mm

Figure 3(c) shows the total pressure distributions for different inlet angles at the cross section of  $X=0$  and  $Z=2000$  mm. The total pressure decreased from the wall to the center of the chamber. This indicated that the vortex transformed static pressure into dynamic pressure. For a given velocity (governed primarily by the inlet velocity), the degree of mixing increased and the total central pressure decreased as the vortex became more intense.

The dynamic pressure distribution was similar to the tangential velocity distribution because the dynamic pressure was directly related to resultant velocity, which was primarily determined by the tangential velocity. Considering the total pressure distributions and the axial and tangential velocity distributions, it was determined that an inlet angle between  $0^\circ$  and  $40^\circ$  was best for a lower swirl, better mixing, and longer residence time in the gas phase.

### Gas-Solid Phase Simulation for the Upper Cyclone High-Temperature Pyrolysis Chamber

Based on the structure of the upper cyclone high-temperature pyrolysis chamber, this section added the rice husk particles for the simulation of the gas-solid phase. To

determine the inlet angle that would result in a longer residence time and better mixing of the particles, a calculation method similar to that for determining the separating efficiency of a cyclone separator was used. The rice husk particles were traced from their release to their final capture. If the solid phase was moving for a longer period of time and the capture efficiency was higher, the structure would have had a higher degree of optimization.

The source of the particle-phase injection was the torus at the top of the upper cyclone chamber. The type of injection was surface injection. The rice husk particles fell at a speed of 0.05 m/s and could escape from the boundary of the outlet. The boundary of the Particle-trajectory Model is "escape," and the cylinder wall condition is "reflect," with a reflection coefficient of 0.8. When the particles hit the bottom of the chamber, they were trapped. The distribution of the rice husk particle diameter was intended to be uniform with a diameter ( $d_p$ ) of 1.3264 mm and a density ( $\rho_p$ ) of 500 kg/m<sup>3</sup>. 6700 particles were considered. It is a Lagrange-Euler method. Table 1 shows the result of the particle trajectories with the varying inlet angles and velocities. The capture efficiency is the percentage of the number of the particles trapped to the total number of the particles traced. When the inlet velocity was either 40 m/s or 80 m/s, the trapping efficiencies were similar for the three inlet angles of 20°, 30°, and 40°. However, when the inlet velocity increased to 120 m/s, the trapping efficiencies dropped significantly with the increasing inlet angles. For a 20° inlet angle, the trapping efficiency increased as the inlet velocity rose, but for 30° or 40°, the trapping efficiency decreased as the inlet velocity increased. Seen from the residence time, all trapped particles had a relatively long residence time of about 2 s, but the particles that escaped had a very short residence time. Therefore, the particles stayed longer and mixed better when the inlet angle was between 20° and 30°, and the inlet velocity was between 40 to 80 m/s. If the particle diameter was not uniform, particles smaller than 0.3 mm would escape and larger than 1 mm would be trapped.

**Table 1.** Simulation Results for the Particle Phase

Inlet angle	Inlet velocity (m/s)	Capture efficiency (%)	Mean residence time for trapped particles (s)	Mean residence time for escaped particles (s)
20°	40	91.21	2.050	0.24360
30°	40	90.74	2.131	0.13910
40°	40	88.14	2.101	0.09875
20°	80	97.61	1.546	0.09421
30°	80	95.61	1.637	0.05584
40°	80	94.17	1.781	0.08030
20°	120	98.41	1.400	0.08428
30°	120	57.45	1.952	0.08701
40°	120	7.5	1.590	0.08194

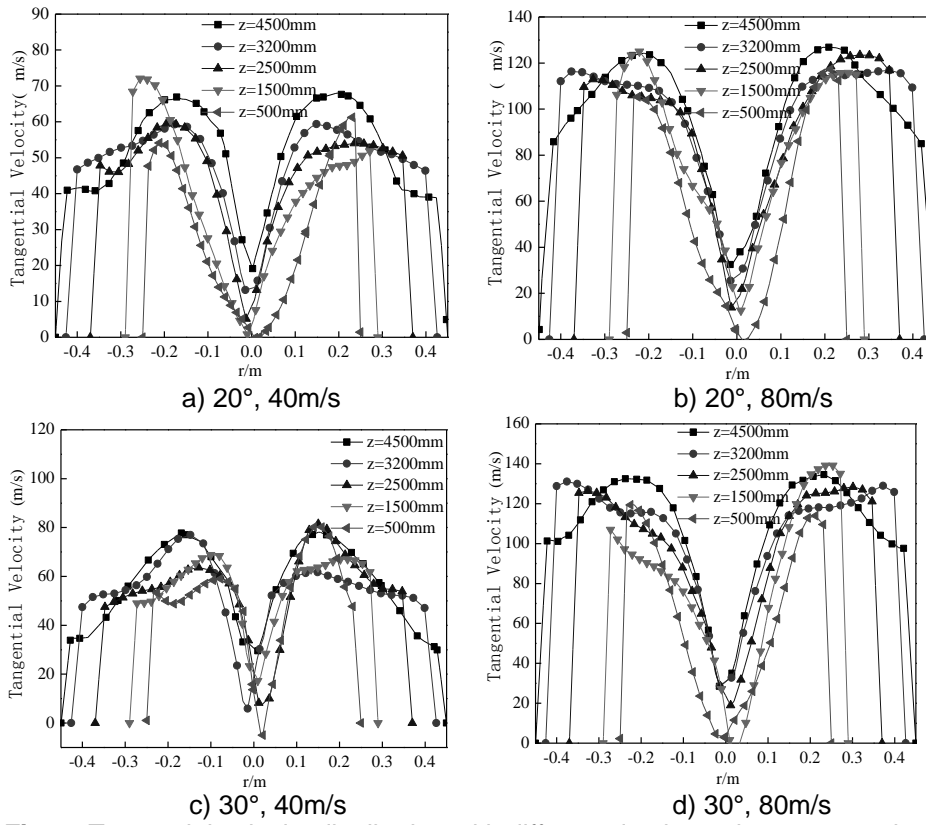


Fig. 4. Tangential velocity distribution with different depths at the cross section of X=0

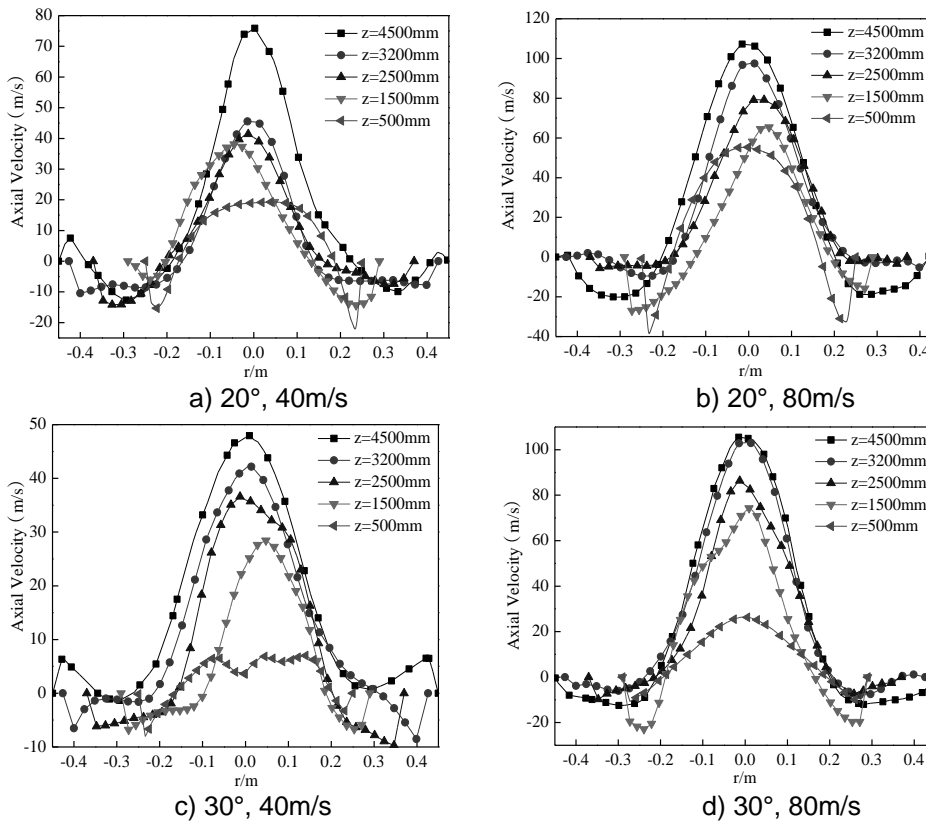


Fig. 5. Axial velocity distribution with different depths at the cross section of X=0

## Gas-Solid Flow Field Simulation for the Entire Two-Stage Rice Husk High-Temperature Pyrolysis and Gasification Cyclone Gasifier

### Results for the gas-phase

There were two gas phases: one was the high-temperature (1600 °C) flue gas that was injected into the upper cyclone chamber at an inlet velocity of 40 m/s or 80 m/s, and the other was the 425 °C steam that was injected into the lower steam spray gasifier. The solid-phase was the rice husk mentioned above.

Figure 4 shows the tangential velocity distribution along the depth at the  $X=0$  cross-section. Compared to the tangential velocity distribution in Fig. 3(b), with rice husk particles and steam injection added, the profiles were less symmetrical. It is because the temperature and velocity of the flue gas and steam were different, and the interaction of the particles and gases led to different turbulence pulsations and vortex core movement. When the inlet velocity was 40 m/s with an inlet angle of 20°, the maximum tangential velocity was much higher than with the 30° inlet angle. This was the opposite tendency to that which occurred when the inlet velocity was 80 m/s.

Figure 5 shows the axial velocity distribution along the depth for the cross section at  $X=0$ . The maximum axial velocity with an angle of 20° was much higher, and the down flow area was much more extensive than with an angle of 30° for both inlet velocities of 40 and 80 m/s, which indicates the enhancement of the mixing and lengthened residence time for pyrolysis and gasification process.

Figures 6 and 7 show the static and dynamic pressure distribution along the depth at  $X=0$ .

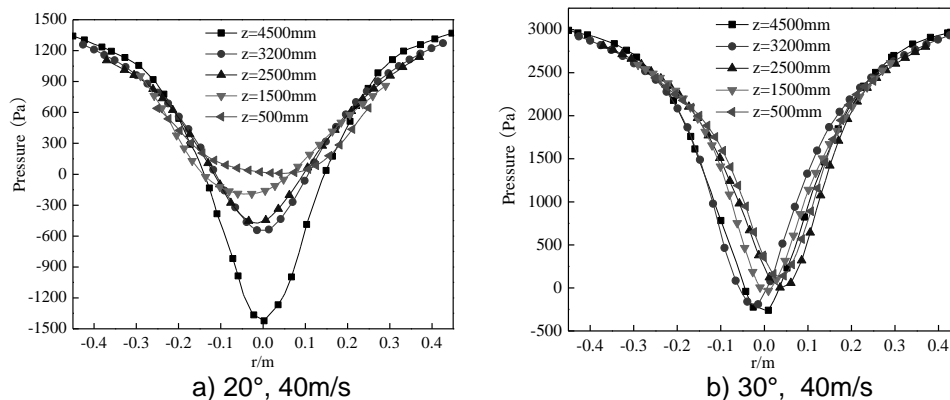


Fig. 6. Static pressure distribution with different depths at the cross section of  $X=0$

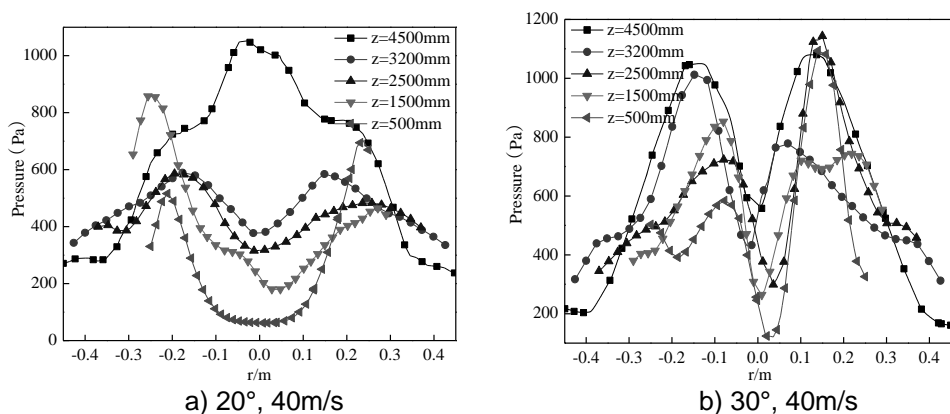


Fig. 7. Dynamic pressure distribution with different depths at the cross section of  $X=0$



For a 30° angle, the low-pressure region in the static pressure distribution near the outlet's central line was much smaller than that for a 20° angle. The dynamic pressure was less symmetrical due to the influence of the resultant velocity, which was primarily determined by the tangential velocity.

#### *Simulation results for the particle phase*

This section investigates the trajectory of uniform diameter particles for inlet angles of 20° and 30° with inlet velocities of 40 m/s and 80 m/s.

**Table 2.** Simulation Results of the Particle Phase

Inlet angle	Inlet velocity (m/s)	Capture efficiency (%)	Mean residence time for the trapped (s)	Mean residence time for the escaped (s)
20°	40	92.85	4.356	0.2131
30°	40	86.87	2.904	0.4096
20°	80	96.88	2.327	0.1367
30°	80	96.75	4.841	0.06532

Table 2 shows the data from the simulation results of the particle phase. The residence time of the trapped particles was more than 2 s for both inlet angles and both inlet velocities. For the escaped particles, the residence time was an order of magnitude less than that of the trapped particles. When the inlet velocity was 40 m/s, the capture efficiency was higher at an angle of 20° than at an angle of 30°. When the inlet velocity was 80 m/s, the capture efficiencies were virtually unaffected for both angles. However, the residence time of the particles trapped with the 30° angle was over twice that of particles with the 20° angle.

## CONCLUSIONS

1. The steam injected into the lower steam spray gasifier had a noticeable influence on the flow field in the upper cyclone high-temperature pyrolysis chamber.
2. The rice husk particles were well mixed and had a longer residence time in the gasifier when the inlet angle was 20° or 30° and the inlet gas velocity was between 40 and 80 m/s.
3. When the inlet velocity was 40 m/s, the capture efficiency with a 20° angle was higher than with a 30° angle. When the inlet velocity was 80 m/s, the capture efficiencies were almost unaffected for both angles, but the residence time of the particles trapped with the angle 30° was over twice that with the 20° angle.

## REFERENCES CITED

- Basu, P. (2010). *Biomass Gasification and Pyrolysis: Practical Design and Theory*, Elsevier, London.
- Devi, L., Ptasiński, K. J., and Janssen, F. J. J. G. (2003). "A review of the primary measures for tar elimination in biomass gasification processes," *Biomass and Bioenergy* 24(2), 125-140. DOI: 10.1016/S0961-9534(02)00102-2

- Fraser, S. M., Abdel-Razek, A. M., and Abdullah, M. Z. (1997). "Computational and experimental investigations in a cyclone dust separator," *Journal of Process Mechanical Engineering* 211(4), 247-257. DOI: 10.1243/0954408971529719
- Gil, J., Corella, J., Aznar, M. P., and Caballero, M. A. (1999). "Biomass gasification in atmospheric and bubbling fluidized bed: Effect of the type of gasifying agent on the product distribution," *Biomass and Bioenergy* 17(5), 389-403. DOI: 10.1016/S0961-9534(99)00055-0
- Knoef, H. A. M. (2005). *Handbook of Biomass Gasification*, BTG Biomass Technology Group, The Netherlands.
- Herguido, J., Corella, J., and Gonzalez-Saiz, J. (1992). "Steam gasification of lignocellulosic residues in a fluidized bed at a small pilot scale: Effect of the type of feedstock," *Industrial and Engineering Chemistry Research* 31(5), 1274-1282. DOI: 10.1021/ie00005a006
- Hu, L., Shi, M., Zhou, L., and Zhang, J. (2004). "Numerical simulation of 3-D strongly swirling turbulent flow in a cyclone separator," *Journal of Tsinghua University Science and Technology* 44(11), 1501-1504.
- Kinoshita, C. M., Wang, Y., and Zhou, J. (1994). "Tar formation under different biomass gasification conditions," *Journal of Analytical and Applied Pyrolysis* 29(2), 169-181. DOI: 10.1016/0165-2370(94)00796-9
- Knight, R. A. (2000). "Experience with raw gas analysis from pressurized gasification of biomass," *Biomass and Bioenergy* 18(1), 67-77. DOI: 10.1016/S0961-9534(99)00070-7
- Liu, Z., Xiao, B., and Yang, J. (2003). "A review of the study of the gas-solid two-phase flow field and the numerical model of cyclone separators," *Journal of Filtration and Separation* 13(1), 42-45.
- Liu, S., Zhang, Y., and Wang, B. (2005). "Cyclone separator three-dimensional turbulent flow-field simulation using the Reynolds stress model," *Transactions of Beijing Institute of Technology* 25(5), 377-379.
- Loppinet-Serani, A., Aymonier, C., and Cansell, F. (2008). "Current and foreseeable applications of supercritical water for energy and the environment," *ChemSusChem* 1(6), 486-503. DOI: 10.1002/cssc.200700167
- Mastellone, M. L., and Arena, U. (2008). "Olivine as a tar removal catalyst during fluidized bed gasification of plastic waste," *AIChE Journal* 54(6), 1656-1667. DOI: 10.1002/aic.11497
- Mettanant, V., Basu, P., and Butler, J. (2009). "Agglomeration of biomass fed fluidized bed gasifier and combustor," *Canadian Journal of Chemical Engineering* 87(5), 656-684. DOI: 10.1002/cjce.20211
- Milne, T. A., Evans, R. J., and Abatzoglou, N. (1998). "Biomass gasifier tars: Their nature, formation, and conversion," TP-570-25357, National Renewable Energy Laboratory, Golden, CO.
- Narváez, I., Orío, A., Aznar, M. P., and Corella, J. (1996). "Biomass gasification with air in an atmospheric bubbling fluidized bed: Effect of six operational variables on the quality of the produced raw gas," *Industrial Engineering Chemistry and Research* 35(7), 2110-2120. DOI: 10.1021/ie9507540
- Pan, Y. G., Roca, X., Velo, E., and Puigjaner, L. (1999). "Removal of tar by secondary air in fluidised bed gasification of residual biomass and coal," *Fuel* 78 (14) 1703-1709. DOI:10.1016/S0016-2361(99)00118-0

- Susanto, H., and Beenackers, A. A. C. M. (1996). "Moving bed gasifier with internal recycle of pyrolysis gas," *Fuel* 75(11), 1339-1347. DOI: 10.1016/0016-2361(96)00083-X
- Sutton, D., Kelleher, B., and Ross, J. R. H. (2001). "Review of literature on catalysts for biomass gasification," *Fuel Processing Technology* 73(3), 155-173. DOI: 10.1016/S0378-3820(01)00208-9
- Zhang, Y., Zhai, M., Dong, P., Jin, H., and Zhu, Q. (2014). "Process simulation for rice husk staging pyrolysis and gasification with steam," *Proceedings of the Chinese Society of Electrical Engineering* 34 (17), 2817-2825. DOI:10.13334/j.0258-8013.pcsee.2014.17.010
- Zhao, C. (2012). *The Numerical Simulation Research on Biomass Pyrolysis and Gasification with High-Temperature in Segmented Gasifier*, M.S. thesis, Harbin Institute of Technology, Harbin, China.

Article submitted: January 15, 2015; Peer review completed: April 12, 2015; Revisions accepted: May 25, 2015; Published: June 4, 2015.

DOI: 10.15376/biores.10.3.4569-4579